THS This is to certify that the

thesis entitled

Preliminary FEM Modeling of Orthogonal Turning

presented by
Alexander Macomb Rucker

has been accepted towards fulfillment of the requirements for

Master of Science degree in Engineering Mechanics

Major professor

Date 5/30/2002

**O**-7639

MSU is an Affirmative Action/Equal Opportunity Institution

## LIBRARY Michigan State University

PLACE IN RETURN BOX to remove this checkout from your record.

TO AVOID FINES return on or before date due.

MAY BE RECALLED with earlier due date if requested.

DATE DUE	DATE DUE	DATE DUE

6/01 c:/CIRC/DateDue.p65-p.15

# PRELIMINARY FEM MODELING OF ORTHOGONAL TURNING

By

Alexander Macomb Rucker

## **A THESIS**

Submitted to
Michigan State University
in partial fulfillment of the requirements
for the degree of

**MASTER OF SCIENCE** 

Department of Mechanical Engineering

2002

### **ABSTRACT**

### PRELIMINARY FEM MODELING OF ORTHOGONAL TURNING

By

### Alexander Macomb Rucker

The purpose of this thesis is to develop a computational model used for studying the effects of changing parameters involved with machining. The information given by the FEM model will ultimately be used in the determination of tool wear. The development of such models are important in the minimization of expensive and time consuming machining experiments for predicting tool life. Finite element method modeling was developed for the computational models for machining of an aluminum alloy (AL319T6) during orthogonal cutting. The model consisted of 2-D, plane strain, reduced integration, and four-nodes bilinear elements with hourglass stiffness control. A ductile fracture criterion based on predetermined distance from the tool tip was applied in ABAQUS to describe crack growth in the chip formation. Chip formation in metal cutting is a large deformation problem. Large deformation of the finite elements was corrected by remeshing the model as needed. The chips predicted by the computational machining model were similar to continuous chips formed in metal cutting. The specific parameters analyzed were the curvature of the formed chip and the reaction forces in the tool during cutting process. Chip curvature and reaction forces are dependant on the rake angle of the tool and the cutting velocity. Curvature of the chip plays a major role in breaking the continuous chip. Reaction forces are important in the design of machine tools and other areas.

## **ACKNOWLEDGEMENTS**

I would like to thank my advisor Dr. Patrick Kwon for the chance to work on this project and for his support and guidance while working on this project.

I would also like to like to thank Tim Wong for all his hard work and late nights he spent on this project. It was very much appreciated.

I would like to acknowledge my family for all their support over my entire college career. Without all your love and support, none of this would have been possible. Thank you.

## **Table of Contents**

Abstract	i
Acknowledgements	iii
List of Figures	<b>v</b> i
List of Tables	viii
Introduction	1
Orthogonal Turning	2
Theory of Metal Machining Applied to Orthogonal Turning	4
Limitations of the Orthogonal Turning Mechanics	9
Introduction to Finite Element Methods	10
Previous Works Using ABAQUS	11
General ABAQUS Methods	12
Components of an ABAQUS Model	14
Units and Coordinate Systems	16
Model Development	17
Modeling in ABAQUS/Explicit	17
Modeling in ABAQUS/Standard	20
Results	26
Sample Calculations for Simplified Mechanics of Orthogonal Turning	26
FEM Results	27
Validation of FEM Model	36

Conclusions	37
Limitations and Future Work	42
References	43
APPENDIX A: Reaction Force vs. Time Plots for Fine Mesh	A1
APPENDIX B: Comparison of Coarse Mesh and Fine Mesh Cutting Force and Thrust Force	B1
APPEXDIX C: Input Files	C1

•

.

.

## **List of Figures**

Figure 1: Orthogonal Turning	3
Figure 2: Two Dimensional Orthogonal Turning Process	3
Figure 3: A View of the Primary and Secondary Shear Zone	4
Figure 4: Geometries of Orthogonal Turning	5
Figure 5: Forces Acting on the Cutting System	6
Figure 6: Relating Reaction Forces	7
Figure 7: Reaction Force Relative to the Work Material	7
Figure 8: Orthogonal Turning	9
Figure 9: Constitutive Relationship for AL316-T6	15
Figure 10: Initial Mesh Analyzed with ABAQUS/Explicit	18
Figure 11: Second Mesh Analyzed in ABAQUS/Explicit	19
Figure 12: Course 2-D Mesh Analyzed in ABAQUS/Standard	21
Figure 13: Mildly Refined Mesh	21
Figure 14: Chip Formation, Remeshing Required	22
Figure 15: Chip Formation, Adaptive Meshing Applied	23
Figure 16: Chip Formation, Cutting Process Continued After Remeshing	23
Figure 17: Finely Refined Mesh Geometry	24
Figure 18: Small Crack Length	25
Figure 19: Large Crack Length	25
Figure 20: Cutting Force vs. Time	29
Figure 21: Thrust Force vs. Time.	29
Figure 22: Cutting Force vs. Rake Angle	30

Figure 23: Thrust Force vs. Rake Angle	31
Figure 24: Cutting Force vs. Cutting Speed	31
Figure 25: Thrust Force vs. Cutting Speed	32
Figure 26: Chip Curvature for chip6b1	33
Figure 27: Chip Curvature for chip6b2	33
Figure 28: Chip Curvature for chip6b3	33
Figure 29: Chip Curvature for chip6b4	34
Figure 30: Chip Curvature for chip6b5	34
Figure 31: Chip Curvature for chip6b6	34
Figure 32: Chip Curvature for chip6b7	35
Figure 33: Chip Curvature for chip6b8	35
Figure 34: Chip Curvature for chip6b9	35
Figure 35: Fine Mesh Cutting Force vs. Time	36
Figure 36: Mild Mesh Cutting Force vs. Time	36
Figure 37: Continuous Chip formed at 0.07 m/s	38
Figure 38: Cutting Force vs. Time Plot at Cutting Speed of 0.07 m/s	39
Figure 39: Thrust Force vs. Time Plot at Cutting Speed of 0.07 m/s	39
Figure 40: Chip Curled into the Work Material	40
Figure 41: Cutting Force vs. Time Plot for Cutting Speed of 0.10 m/s	41
Figure 42: Thrust Force vs. Time Plot for Cutting Speed of 0.10 m/s	42

## **List of Tables**

Table 1: Cutting Parameters of Mildly Refined Mesh2	8
Table 2: Cutting Parameters for Finely Refined Mesh2	8
Table 3: Summary of Results for Reaction Forces	9

## Introduction

Great bounds in machining research have been made in the past decade.

These achievements have been mainly due to the ability to establish reliable theories and incorporate these theories into a finite element analysis to predict important cutting parameters. The parameters include reaction forces (cutting forces), chip formation and curvature, and cutting temperatures. These parameters have to be used to evaluate surface finish, tool wear and tool life in a more scientific approach to machining studies. Finite element analysis minimizes expensive and time-consuming gathering of experimental machining information. Finite element analysis has been performed and discussed in this thesis. This analysis is the preliminary physical modeling of machining and does not incorporate temperature effects into the material constitutive equation.

Prediction of reaction forces achieved during the cutting process is important for machine design and cutting tool design, as well as for the control and optimization of different machining processes. It is also important that material behavior during chip formation is understood in terms of cutting conditions. The material constitutive equation is an important key in obtaining interfacial conditions. However, it is beyond the scope of this thesis.

Chip curvature plays a major role in breaking the continuous chip. This gives information about material removal and is important in machining operations.

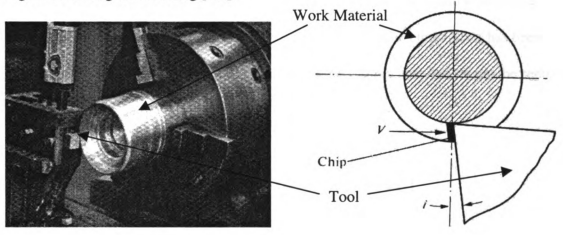
Machining is a very important manufacturing process. It can be applied to virtually all metals. Machining can be used to produce many different geometries, ranging from simple to very complex. Dimensions of these geometries can be created at very close tolerances with smooth surface finishes. Because machining is so widely used, it is of much interest to better describe the phenomenon that takes place during the machining process.

Machining is a manufacturing process in which a cutting tool is used to remove excess material from the work piece so that a desired shape is formed. The cutting action involves primarily shear deformation of the work material for the formation of the metal chip during machining material removal process.

## **Orthogonal Turning**

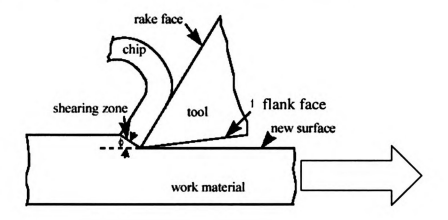
The preliminary model discussed in this thesis was developed to simulate orthogonal metal cutting (orthogonal turning). Orthogonal turning is a metal cutting operation in which the work material consists of a cylindrical tube rotating on a lathe and the cutting tool is brought into contact perpendicular to the work material (See Figure 1). The work material, as it is being sheared off to form the chip, can be directly observed.

Figure 1: Orthogonal Turning [6,7]



Orthogonal turning can be simplified in two dimensions (See Figure 2).

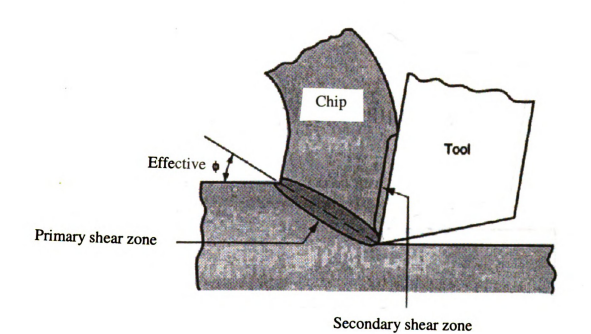
Figure 2: Two Dimensional Orthogonal Turning Process [1]



In Figure 2, the cutting tool has an ideally sharp cutting edge, which serves to separate a chip off of the work material. The tool has two faces of interest defined as the rake face and the flank face. The rake face generates the chip and directs the flow of the chip. The flank face allows for clearance of the tool to protect the newly formed work surface.

The shear deformation of the work material occurs along a thin zone called the primary shear zone. Another shearing action occurs in the chip after it has been formed in the secondary shear zone. Primary and secondary shear zones can be seen in Figure 3.

Figure 3: A View of the Primary and Secondary Shear Zone [1]



#### Theory of Metal Machining Applied to Orthogonal Turning

The most important reason to carry out orthogonal turning is because it is relatively simple to model with simplified mechanics equations. Orthogonal turning is one of two main models used for studying constitutive relationships at extremely high strain rates.

From the two-dimensional simplified view of orthogonal turning (Figure 2), the geometry of the process involved can be described by a series of angles (See Figure 4).

Figure 4: Geometries of Orthogonal Turning [1]

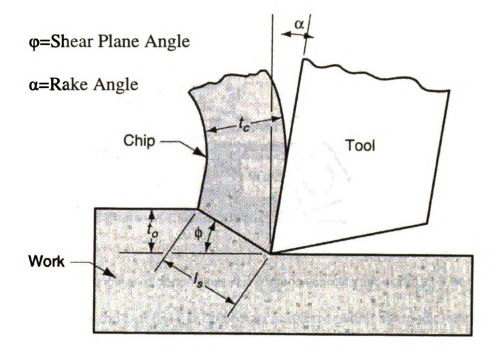
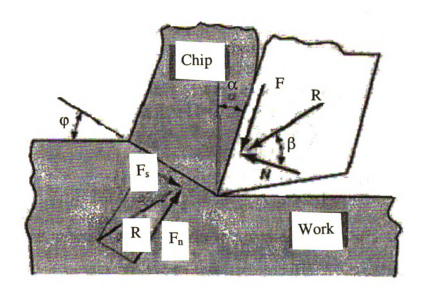


Figure 4 shows the work material being cut by the tool. The rake angle  $(\alpha)$  is the angle of the rake face of the tool from a vertical axis. Since the primary shear zone is thin, it can be assumed to be a plane, called the shear plane angle. The shear plane angle  $(\phi)$  is the approximate angle at which shear failure of the material takes place. The original chip thickness  $(t_0)$ , deformed chip thickness  $(t_0)$ , and length of the

shear plane (I<sub>s</sub>) are also included. A description of the forces acting on the system can be seen in Figure 5.

Figure 5: Forces Acting on the Cutting System [1]



There are various ways to decompose the force involved with cutting. The reaction force relative to the tool (R) can be broken into force acting along the rake face (F), and force acting normal to the rake face (N). The reaction force relative to the shear plane (R') can be broken into force acting along the shear plane ( $F_a$ ), and force acting normal to the shear plane ( $F_a$ ). These forces can then be related (Figure 6) to a reaction force relative to the work material (See Figure 7).

Figure 6: Relating Reaction Forces [1]

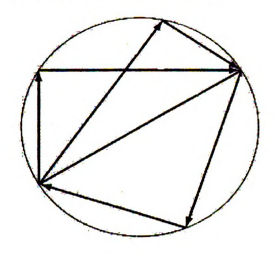
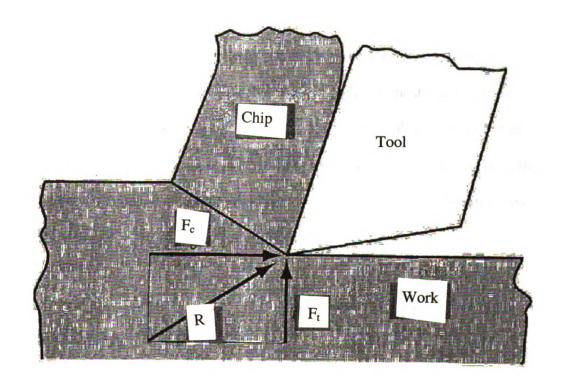


Figure 7: Reaction Force Relative to the Work Material [1]



The reaction force is now relative to the work material, which is described as a cutting force (Fc), and a thrust force (Ft). These forces are approximated by the Merchant Equation [1].

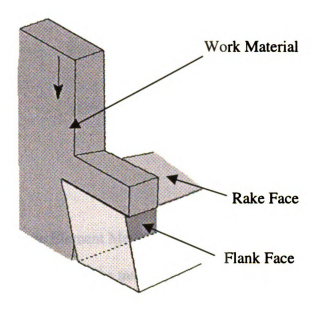
-The Cutting Force: 
$$F_c := \frac{\tau_{xy} \cdot t_0 \cdot \cos(\beta - \alpha)}{\sin(\phi) \cdot \cos(\phi + \beta - \alpha)}$$

-The Thrust Force: 
$$F_t := \frac{\tau_{xy} \cdot t_0 \cdot \sin(\beta - \alpha)}{\sin(\phi) \cdot \cos(\phi + \beta - \alpha)}$$

Where  $\tau_{xy}$  is the shear stress at the yield point (perfectly plastic material assumed).

Orthogonal turning is also used because it provides reasonably good modeling of chip formation along the major cutting edge of most major cutting operations. These other cutting operations include turning, milling, drilling (See Figure 8), and other conventional machining operations. In orthogonal turning, the cutting speed is uniform along the rake face. However, in drilling, the cutting speed is directly related to the distance from the center axis of the drill.

Figure 8: Orthogonal Turning



Orthogonal turning is also extremely useful because it is a very open and exposed process. This allows experimental data to be obtained much more easily than cutting operations that are closed to the environment. Plans for carrying out experiments at NIST are being made as the current models improve.

#### **Limitations of the Orthogonal Turning Mechanics**

The Merchant Equation assumes that the shear strength of the work material is a constant that is unaffected by strain rate and temperature. These assumptions are not obeyed in practical machining operations. Therefore, the Merchant Equation is considered to be an approximate relationship of terms, rather than a precise mathematical statement. This is the main incentive for Finite Element Methods.

# Introduction to Finite Element Methods

Finite Element Methods are used for the local estimation of tractions (stress) and temperatures during the machining process. The evaluation of these parameters allows for a prediction of tool wear. The work done in this thesis was to develop a preliminary machining model, into which a better constitutive model can be incorporated in future work.

The first step of any finite element simulation is to discretize the actual geometry of the structure using a collection of finite elements. Each finite element represents a discrete portion of the physical structure. Shared nodes and edges join the finite elements. The collection of nodes and finite elements is called the mesh. The number of elements used in a particular mesh is referred to as the mesh density. In a stress analysis, displacements of the nodes are the fundamental variables calculated. Once the nodal displacements are known, the stresses and strains in each finite element can be determined. At any other point in the element, the displacements are obtained by interpolating from the nodal displacements.

AAA	AAA	BBBBBBBBB		AAA	AAA	QQ	QQQQQ	Q	U	U	SSSSSSS	
A	A	В	В	A	A	Q		Q	U	U	S	
A	A	В	В	A	A	Q		Q	U	บ	S	
A	A	В	В	A	A	Q		Q	U	U	S	
AAAAA	AAAAA	BBBBB	BBBB	ааааааааа		Q Q		Q	U	U	SSSSSSS	
A	A	В	В	A	A	Q	Q	Q	U	บ	S	
A	A	В	В	A	A	Q	Q	Q	U	U	S	
A	A	В	В	A	A	Q	Q	Q	U	U	S	
A	A	BBBBB	BBBBB	A	A	QQ	QQQQQ	Q	זטטט	טטטטט	SSSSSSS	
								Q				

< <	<b>&gt;</b>   <b>&gt;</b> 	< <	>   > 	< <	<b>&gt;</b>   <b>&gt;</b>	< <	>   > 	< <	>   > 	< <	<b>&gt;</b>   <b>&gt;</b> 	< <	<b>&gt;</b>   <b>&gt;</b>	<	<b>&gt;</b>   <b>&gt;</b>	<	<b>&gt;</b>   <b>&gt;</b>	<	<b>&gt;</b>     <b>&gt;</b>
						·	·	·	- <del>-</del> -	·	·								
	l	<	>		1	<	>		ı		l	<	>	< < < <	>	<	>	<	>
	İ	<	<b> </b> >				İ		j		İ		ĺ	<	>	<	>	<	>
<	>		ĺ	<	>		İ	<	>	<	>		ĺ	<	>			<	>
<	>		ĺ	<	>	<	>	<	>	<	>	<	>	<	>				ĺ
<	>	<	<b> </b> >	<	>	<	>	<	>	<	>	<	>		Ì	<	>		ĺ
<	>	<	<b> </b> >	<	>	<	>	<	>	<	>	<	>		Ì	<	>	<	>
														<					

## **Previous Works Using ABAQUS**

Many machining researchers have developed their own finite element code to model orthogonal turning [9-13]. Only two previous works could be found using ABAQUS to model orthogonal turning.

Komvopoulos and Erpenbeck [4] used a chip-separation criterion based on distance from tool. This is presumed to be a specified crack length for a given time. The model was assumed to be quasi-static so that initial inertial effects of the simulation could be ignored.

Lei et al. [5] also used a chip-separation criterion based on distance from tool, which was presumed to be the specified crack length for a given time. The tool-chip

interaction was modeled by small-sliding contact. Rezoning of the mesh (remeshing) was also used in this paper. It was presumably done with the aid of ABAQUS/CAE, which is a windows environment that allows for model development (Michigan State University does not own a license for ABAQUS/CAE). A user-defined constitutive relation for flow stress was incorporated into the material definition.

## **General ABAQUS Methods**

ABAQUS is a set of powerful engineering simulation programs, based on the finite element method [3,4]. A nonlinear analysis was used in this thesis. ABAQUS automatically chooses appropriate load increments and convergence tolerances. Not only does it choose the values for these parameters, it also continually adjusts them during the analysis to ensure that an accurate solution is obtained efficiently.

ABAQUS/Standard was utilized for the majority of the analyses described in this thesis. ABAQUS/Standard is a general-purpose analysis module that can solve nonlinear problems [3,4]. A complete ABAQUS/Standard analysis usually consists of three distinct stages: preprocessing, simulation, and post processing.

### Preprocessing

In the preprocessing stage, the model of the physical problem must be defined and an ABAQUS input file must be created. This was done directly using a text editor.

The simulation is where ABAQUS formulates results. An element's formulation refers to the mathematical theory used to define the element's behavior. All elements used are based on the Lagrangian or material description of behavior [3,4]. This means

that the material associated with an element remains associated with the element throughout the analysis. Two dimensional plane strain elements were used in this thesis because the thickness of the formed chip is thin compared to the thickness of the work material. Plane strain elements assume that the out-of-plane strain is zero. This infers that they are used to model thick structures.

ABAQUS uses numerical techniques to integrate various quantities over the volume of each element. Using Gaussian Quadrature, ABAQUS evaluates the material response at each integration point in each element [3,4]. Reduced integration elements were used in this thesis.

Reduced integration elements have a single integration point located at the centroid of the element. At this point, average values of the strain components are computed for the element. This was done to prevent the elements from being too stiff and shear locking to occur. Shear locking means that strain energy is creating shearing deformation rather than the intended bending deformation, so the overall deflections are less.

The objective of the analysis is to determine this response. ABAQUS uses the Newton-Raphson method to obtain solutions for nonlinear problems [3,4]. In a nonlinear analysis the solution cannot be calculated by solving a single system of equations.

Therefore, the solution is found by applying specified loads gradually, and incrementally working toward a final solution. ABAQUS breaks the simulation into a number of load increments and finds the approximate equilibrium configuration at the end of each load increment. Each increment is composed of many iterations. For each iteration,

ABAQUS forms the model's stiffness matrix and solves a system of equations. This

means that each iteration is equivalent, in computational cost, to conducting a complete linear analysis. The sum of all of the incremental responses is the approximate solution for the nonlinear analysis.

## Post Processing

During post processing, the results can be evaluated once the simulation has been completed and the displacements, stresses, or other fundamental variables have been calculated. ABAQUS/Viewer provides a tidy compilation of large amounts of data, which aids in the evaluation of results.

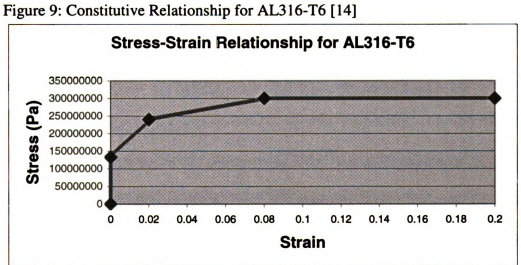
## Components of an ABAQUS Model

An ABAQUS model is composed of several different components that together describe the physical problem to be analyzed and the results to be obtained. The model must contain the following information: geometry, material data, loads and boundary conditions, and analysis type.

Initially, the geometry must be generated. Finite elements and nodes define the basic geometry of the physical structure being modeled in ABAQUS. Each element in the model represents a discrete portion of the physical structure, which is, in turn, represented by many interconnected elements. Shared nodes connect elements to one another. The coordinates of the nodes and the connectivity of the elements make up the model geometry. The collection of all the elements and nodes in a model is called the mesh. The mesh is only an approximation of the actual geometry of the structure. The element type, shape, and location, as well as the overall number of elements used in the

mesh, affect the results obtained from a simulation. In general, the greater the mesh density is, the more accurate the results. As the mesh density increases, the analysis results are likely to converge to a unique solution, and the computer time required for the analysis increases. The solution obtained from the numerical model is generally an approximation to the solution of the physical problem being simulated. The extent of the approximations made in the model's geometry, material behavior, boundary conditions, and loading determines how well the numerical simulation matches the physical problem.

Because displacements of the nodes are the fundamental variables calculated, it is important to have accurate material data for the calculation of other variables. Material properties for all elements must be specified. While high-quality material data are often difficult to obtain, particularly for the more complex material models, the validity of the ABAQUS results is limited by the accuracy and extent of the material data. The material AL319-T6 was used for the models developed in this thesis. Material data supplied from General Motors was used and the simplest constitutive relationship is for AL316-T6 is shown in Figure 9.



Boundary conditions are used to constrain portions of the model to remain fixed (zero displacements) or to move by a prescribed amount (nonzero displacements). In a static analysis, enough boundary conditions must be used to prevent the model from moving as a rigid body in any direction; otherwise, unrestrained rigid body motion causes the stiffness matrix to be singular.

An ABAQUS simulation can generate a large amount of output. To avoid using excessive disk space, a node output frequency was used to limit the output to that required for interpreting the results. Output was recorded at the frequency specified.

## **Units and Coordinate Systems**

Before starting to define this or any model, you need to decide which system of units you will use. ABAQUS has no built-in system of units. All input data must be specified in consistent units. Standard Metric Units were used (Newton's, meters).

The default global coordinate system in ABAQUS is a right-handed, rectangular (Cartesian) system.

## **Development of Finite Element Model**

Machining is a difficult process to model because of the failure of the material and large deformations of the chip occurring. At steady states, a rigid surface (the tool) traveled at a constant velocity into a mesh of elements (the work material), causing them failure. These large displacements and large deformations in the mesh are difficult to model. In order for the chip to form, mesh failure along certain nodes must take place. If no mesh failure takes place, the rigid surface will not penetrate the mesh and the mesh will react like a balloon poked by a finger. Therefore, it is imperative to be able to control failure of the mesh and apply a failure criterion at specific points of the mesh. The problem of having a chip form while the tool contacted the material was considered several ways.

## Modeling in ABAQUS/Explicit [4]

Initially, ABAQUS/Explicit was utilized for the modeling of machining. The motivation behind this was mainly so the adaptive mesh option could be incorporated into the model. The adaptive mesh option is desirable because it automatically corrects for large deformations of elements, allowing for the simulation to be more accurate and run longer. However, the failure of the mesh was difficult to implement in ABAQUS/Explicit.

It was attempted to include an element deletion option based on shear failure.

This option was applied where the mesh was expected to fail. This was on a thin layer of elements that connected the chip elements to the rest of the work material. Initially, a

very soft material with much lower material properties was specified for this thin layer of elements so that failure would occur rather easily. This soft material was defined in the user subroutine VUMAT defined. A three dimensional, 200,000-element mesh was constructed that was 16 elements in height, 50 elements thick, and 250 elements in length (See Figure 10).

Figure 10: Initial Mesh Analyzed with ABAQUS/Explicit



It can be seen from Figure 10 that the chip is much too stiff and is behaving similar to a rigid body. This can be explained by the large difference in material properties of the soft connecting layer. A problem can be seen as the rear end of the chip is penetrating the rest of the model. Even though the failed elements are still being

shown, it can be seen that they are carrying zero stress. Due to the large size of the mesh, it took much too long to process this simulation (nearly a day).

Another mesh was created that was much smaller in size to cut down on processor time. This was a three dimensional, 1,000-element mesh that was 5 elements in height, 5 elements in thickness, and 40 elements in length (See Figure 11). In addition to the variation in the number of elements, added boundary conditions (fixation in the Y-direction) were added to the rear end nodes of the work material to prevent penetration of the chip layer into the rest of the work material.

Figure 11: Second Mesh Analyzed in ABAQUS/Explicit

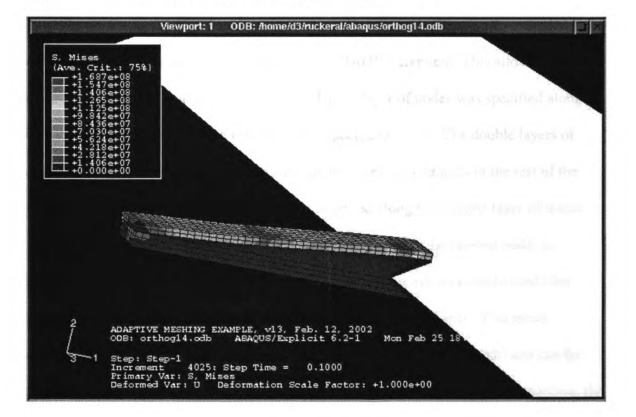


Figure 11 shows the chip still behaving much too rigidly, because of the soft layer of material. It can be seen that the additional boundary conditions to the rear end of the work material corrected the previous penetration problem. The soft material layer is still failing very easily and carries no stress.

The next step was to make the material properties of the thin connecting layer of elements similar to those of the rest of the work material. When this request was made in the user subroutine, the ABAQUS analysis would not run. After ABAQUS/Explicit attempts were exhausted, focus was switched to the use of ABAQUS/Standard.

## Modeling in ABAQUS/Standard [3]

A major motivation for the use of ABAQUS/Standard is that it allows for the use of fracture mechanics, which is not allowed in ABAQUS/Explicit. This allows for the modeling of material failure in the mesh. A double layer of nodes was specified along the surface where failure of the material was expected to occur. The double layers of nodes were defined to be initially bonded, bonding the chip elements to the rest of the work material. A ductile failure criterion was applied along this double layer of nodes. As the tool progresses, a crack length was specified, allowing the bonded nodes to separate and the chip to form. A coarse two-dimensional mesh was constructed (See Figure 1) to apply the fracture mechanics options in a timely manner. This mesh consisted of 200 elements (5 elements in height and 40 elements in length) and can be seen in Figure 12. Once the fracture mechanics options were used with some success, the mesh was mildly refined (See Figure 13). An offset of the first few elements was

included to make the model initially less stiff, giving the simulation a greater chance of running.

Figure 12: Course 2-D Mesh Analyzed in ABAQUS/Standard

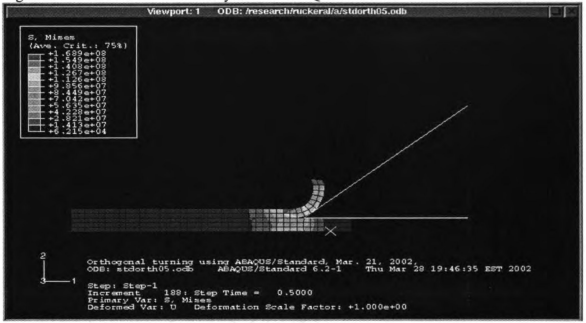
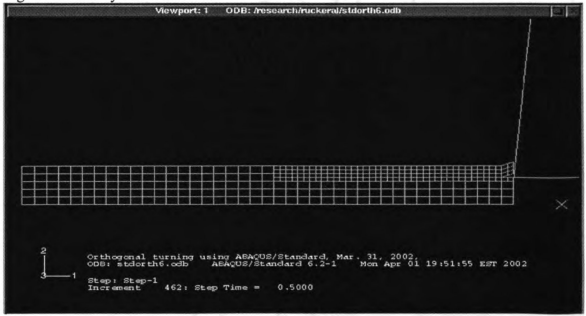


Figure 13: Mildly Refined Mesh



As the simulation proceeded in ABAQUS/Standard, the chip formed and data was recorded. During the simulation, large deformations of the elements were evident (See Figure 14). The simulation would stop once elements became severely distorted. The increment was noted when elements approached severe distortion as seen through ABAQUS/Viewer. In order to correct these highly distorted elements, data was imported from the specified increment into ABAQUS/Explicit. An adaptive meshing option was applied with a Lagrangian constraint (See Figure 15) to the mesh, correcting the severely distorted elements.

The data was then imported back into ABAQUS/Standard after the first increment in ABAQUS/Explicit. The simulation was then continued (See Figure 16) to the end of the simulation or until the remeshing process needed to be repeated.

Viewport: 1 ODB: hesearthruckeral/starth6.odb

Figure 14: Chip Formation, Remeshing Required

Figure 15: Chip Formation, Adaptive Meshing Applied

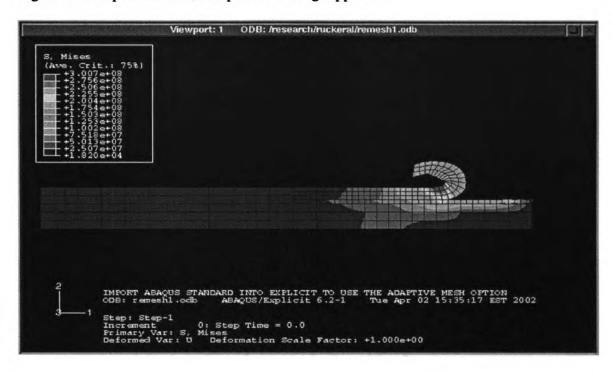


Figure 16: Chip Formation, Cutting Process Continued After Remeshing



Once these operations were carried out with the course mesh, the next step was to greatly refine the mesh. A new mesh was created (see Figure 17) consisting of a total of 4,000 elements (16 elements in height and 250 elements in length). In addition to the refinement in element size, crack tip location was also refined. It was seen that large element deformations did not occur for the fine mesh simulations. Therefore, remeshing was not needed.



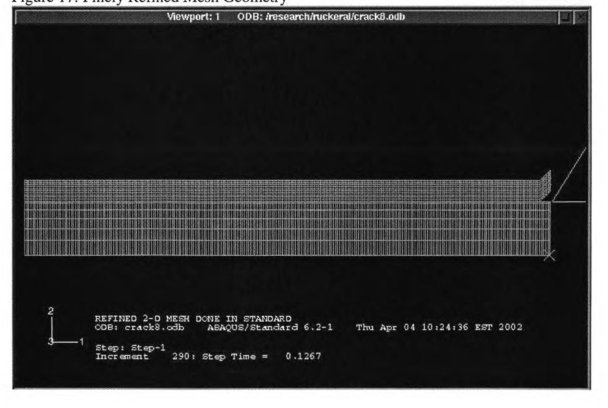


Figure 18 and Figure 19 show the difficulty in correctly specifying the crack length. The crack opening is desired to be as close to the tool tip as possible to model what is happening in reality of the machining process. Initially, if the crack length is not large enough, the crack will not be allowed to open and the tool will crash into unopened

nodes (Figure 18), stopping the analysis. Also, the crack opening must initially be larger than what is actually observed in machining. This is because if the model is initially too stiff, the simulation will terminate. If a large crack opening is specified (Figure 19), the analysis will be allowed to run, but what is modeled does not resemble the actual machining process.



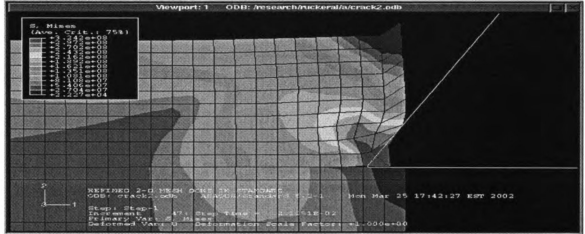
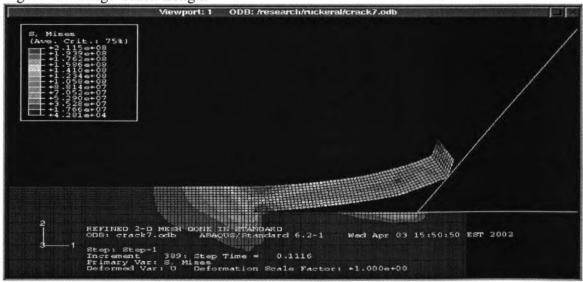


Figure 19: Large Crack Length



Once an acceptable crack length vs. time was established, results were taken.

## **Results**

Results were calculated according to the Merchant Equation [1] to obtain an approximate solution.

# Sample Calculations for Simplified Mechanics of Orthogonal Turning:

-Calculations made for a ten degree rake angle

Cutting Force (N): 
$$F_{cut} := \frac{\tau_{y} \cdot t_{o} \cdot w \cdot \cos(\beta - \alpha)}{\sin(\phi) \cdot \cos(\phi + \beta - \alpha)}$$

Thrust Force (N): 
$$F_{\text{thrust}} := \frac{\tau_{y} \cdot t_{o} \cdot w \cdot \sin(\beta - \alpha)}{\sin(\phi) \cdot \cos(\phi + \beta - \alpha)}$$

Where:

Young's Modulus (Pa): E := 73000000000

Poisson's Ratio: v := .33

Axial Yield Stress (Pa):  $\sigma_y := 133000000$ 

 $\tau_y := \sqrt{\frac{2}{3}} \cdot \sigma_y$   $\tau_y = 1.08610^8$ 

Shear Yield Stress (Pa):

Width (m): w := 1

 $\phi := 18 \cdot \frac{\pi}{180}$ Shear Plane Angle (Rad):

Original Chip Thickness (m):  $t_0 := .006$ 

$$\alpha := 10 \cdot \frac{\pi}{180}$$
 Rake Angle (Rad):

$$\beta := 64 \cdot \frac{\pi}{180}$$

Beta Angle (Rad):

Results (in Newton's): 
$$F_{cut} = 4.011 \cdot 10^6 \, \text{s}$$
  $F_{thrust} = 5.52 \cdot 10^6 \, \text{s}$ 

It is important to note that the forces are very high. This is because some of the assumed parameters are unrealistic. For instance, a machined chip of six millimeters is very large. Original chip thickness is commonly on the order of tenths of a millimeter.

Also, a width of one meter is extremely large. It is usually along the order of millimeters. This width was used because the FEM model uses plane strain, which assumes a thickness of one.

The results obtained from the Merchant Equation are an approximation of the forces involved in the machining process modeled by FEM in this thesis. These results were used to determine if the FEM results were along the same order of magnitude as these simplified equations. FEM results are expected to be more accurate.

### **FEM Results**

Results were recorded for three different rake angles (10°, 15°, 20°) at three different cutting speeds (70mm/sec, 100mm/sec, 130 mm/sec) for the finely refined mesh (Figure 17). Results were also recorded for the mildly refined mesh (Figure 13) to show similarities of results. Table 1 and Table 2 shows the cutting parameters associated with

the ABAQUS file name for the mildly meshed model and the finely meshed model, respectively. Each simulation for files chip6b1-9 took approximately 15 hours to run.

Table 1: Cutting Parameters of Mildly Refined Mesh

File Name	Rake Angle (deg)	Cutting Speed (m/sec)	Chip Thickness (m)
res1	10	0.07	0.006
res2	15	0.07	0.006
res3	20	0.07	0.006
res4	10	0.1	0.006
res5	15	0.1	0.006
res6	20	0.1	0.006

Table 2: Cutting Parameters for Finely Refined Mesh

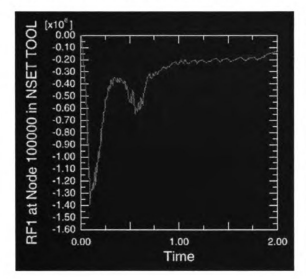
File Name	Rake Angle (deg)	Cutting Speed (m/sec)	Chip Thickness (m)	
chip6b1	10	0.07	0.006	
chip6b2	15	0.07	0.006	
chip6b3	20	0.07	0.006	
chip6b4	10	0.1	0.006	
chip6b5	15	0.1	0.006	
chip6b6	20	0.1	0.006	
chip6b7	10	0.13	0.006	
chip6b8	15	0.13	0.006	
chip6b9	20	0.13	0.006	

The cutting forces and thrust forces were recorded for each of the files. Chip curvature was also noted for general comparison.

Reaction forces were estimated from the force versus time plots when the curves leveled off and reached an approximate steady state (See Figure 20 and Figure 21). Table 3 and shows a summary of results for the reaction forces (cutting force and thrust force) for the fine mesh. All reaction force versus time plots is included in APPENDIX: A.

Figure 20: Cutting Force vs. Time

Figure 21: Thrust Force vs. Time



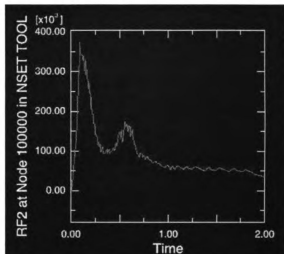


Table 3: Summary of Results for Reaction Forces

File Name	Rake Angle (deg)	Cutting Speed (m/sec)	Cutting Force (N)	Thrust Force (N)
chip6b1	10	0.07	250000	55000
chip6b2	15	0.07	200000	70000
chip6b3	20	0.07	150000	90000
chip6b4	10	0.1	700000	200000
chip6b5	15	0.1	600000	225000
chip6b6	20	0.1	500000	250000
chip6b7	10	0.13	650000	150000
chip6b8	15	0.13	550000	175000
chip6b9	20	0.13	500000	200000

An incremental decrease of cutting force can be seen with and increasing rake angle at all three cutting speeds (Figure 22). An incremental increase in cutting force can be seen with and increasing rake angle at cutting speeds of 0.07 m/sec and 0.10 m/sec (Figure 23). There is also and incremental increase in cutting force and thrust force at all three cutting speeds for rake angles of 10 deg. and 15 deg. (Figures 24 and 25).

Figure 22:

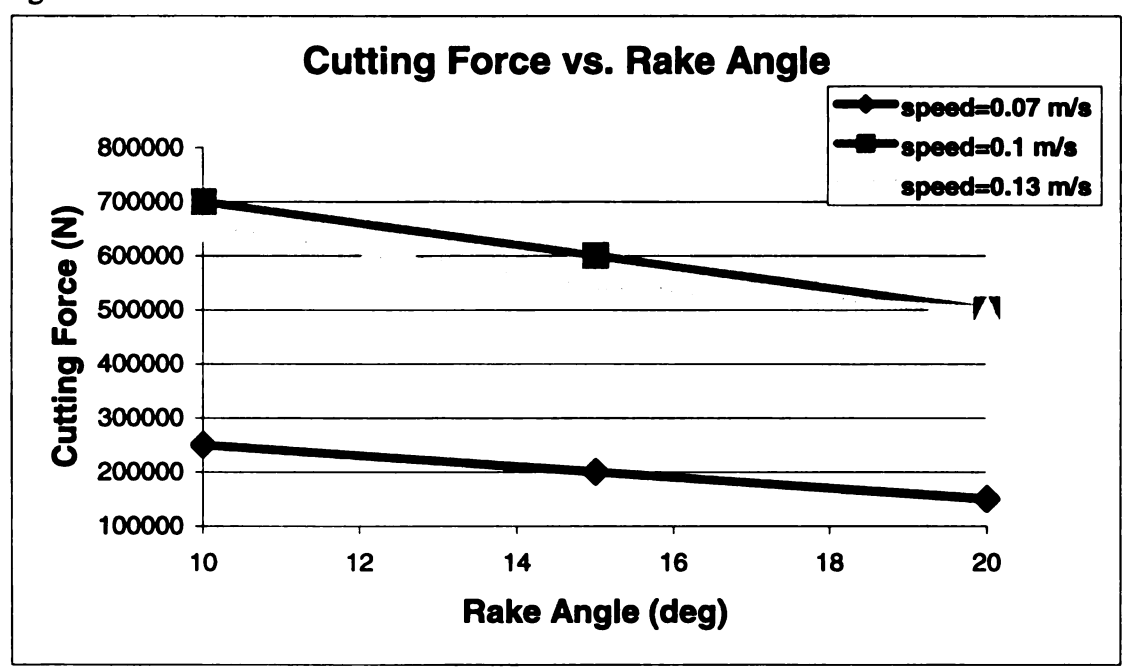


Figure 23:

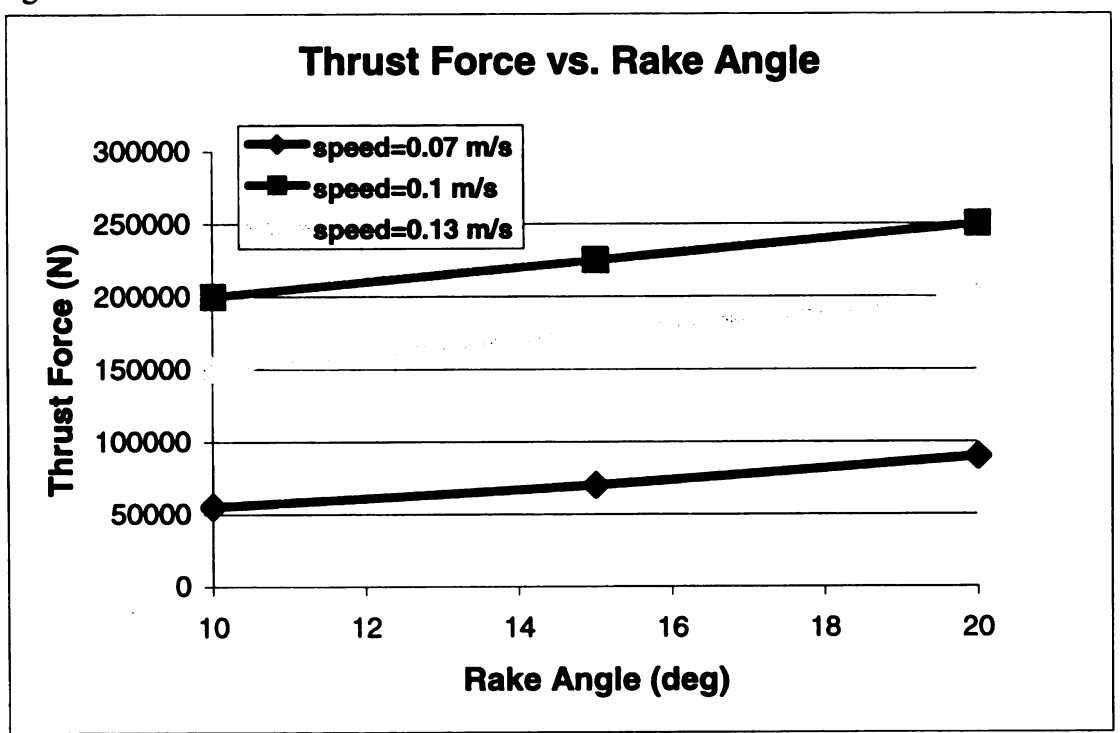


Figure 24:

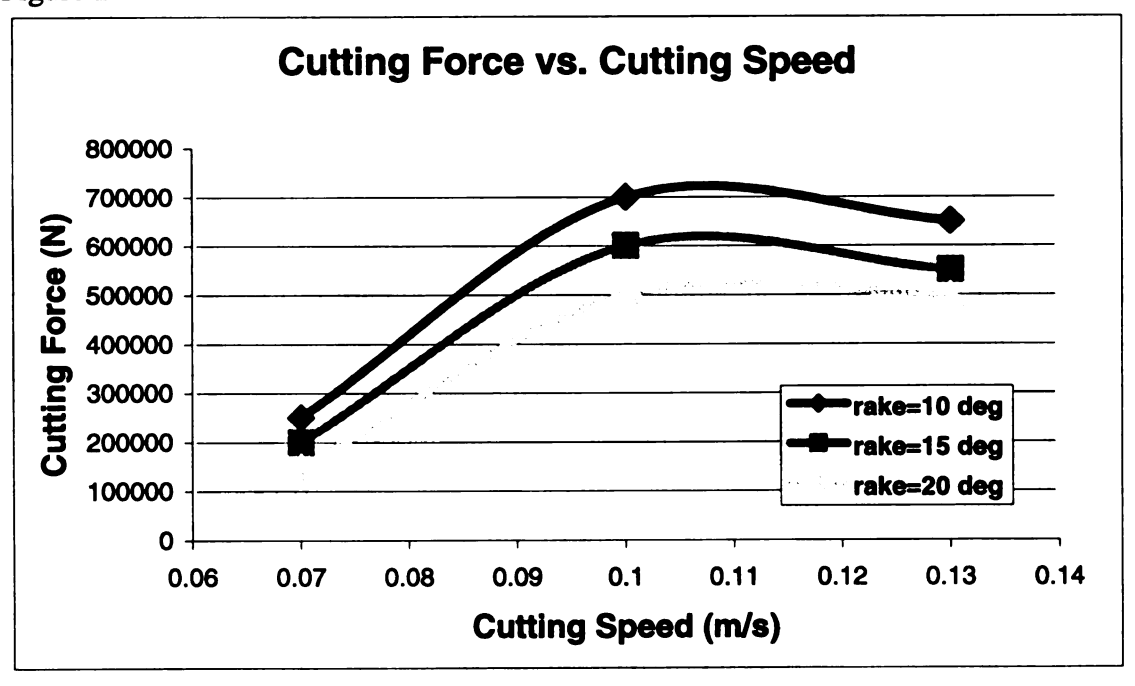
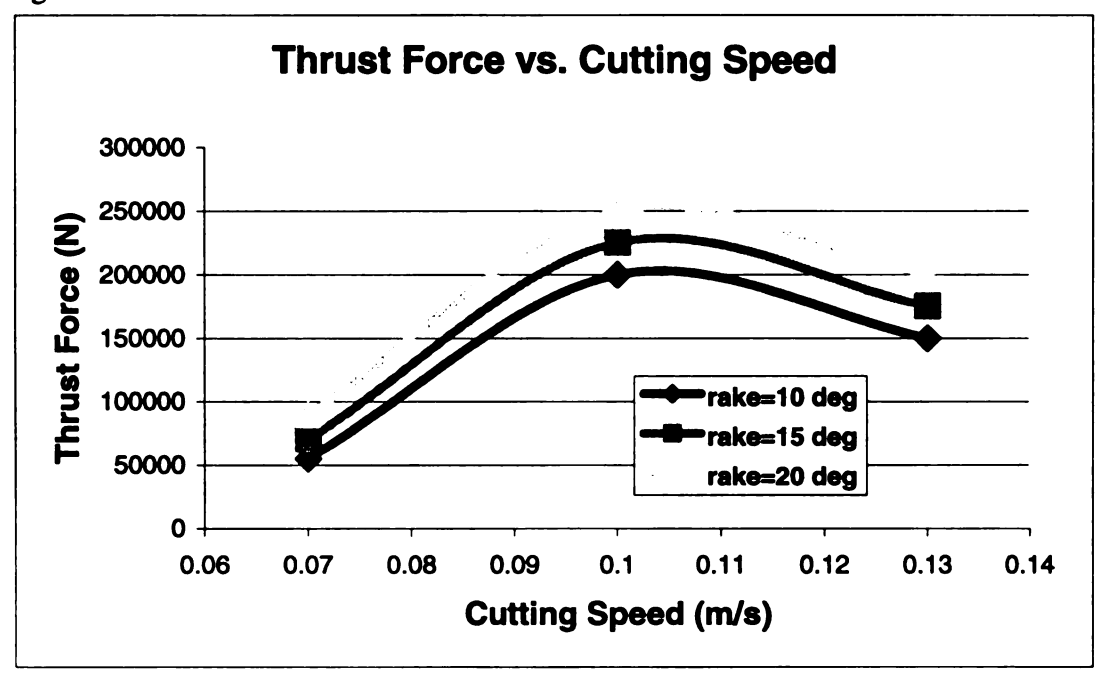


Figure 25:



# Chip Curvature

The chip curvatures were noted at a constant cutting distance of 0.028 m for each of the files. This was done because it is easiest to view chip curvature and changes in chip curvature at the beginning of the analysis. Figures 22 to 30 show chip curvatures for each of the finely meshed models.

Figure 26: Chip Curvature for chip6b1



Figure 27: Chip Curvature for chip6b2



Figure 28: Chip Curvature for chip6b3



It can be seen that chip6b1 (Figure 26) has more curvature that chip6b2 (Figure 27) and chip6b2 has more curvature than chip6b3 (Figure 28).

Figure 29: Chip Curvature for chip6b4

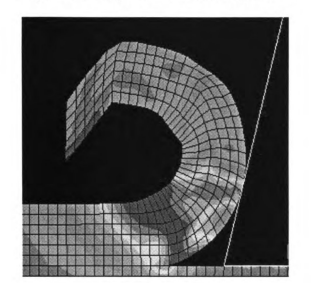


Figure 30: Chip Curvature for chip6b5

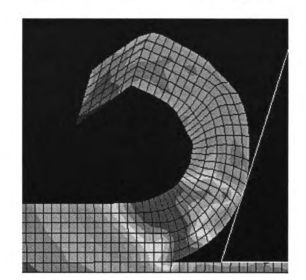
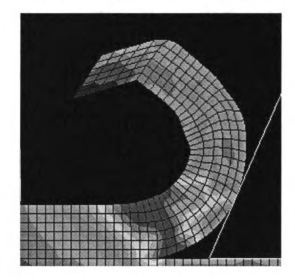


Figure 31: Chip Curvature for chip6b6



It can be seen that chip6b4 (Figure 29) has more curvature that chip6b5 (Figure 30) and chip6b5 has more curvature than chip6b6 (Figure 31). It can also be seen that chip6b4 has more curvature than chip6b1, chip6b5 has more curvature than chip6b2, and chip6b6 has more curvature than chip6b3.

Figure 32: Chip Curvature for chip6b7

Figure 33: Chip Curvature for chip6b8





Figure 34: Chip Curvature for chip6b9



It can be seen that chip6b7 (Figure 32) has more curvature that chip6b8 (Figure 33) and chip6b8 has more curvature than chip6b9 (Figure 34).

#### Validation of FEM Model

It can be seen that the FEM results are on the same order of magnitude as the results from the Merchant Equation. This shows that the FEM model is generating somewhat realistic results.

It can be seen from Figures 35 and 36 that the reaction forces generated from the fine mesh and the mildly refined mesh are similar.

Figure 35: Fine Mesh Cutting Force vs. Time

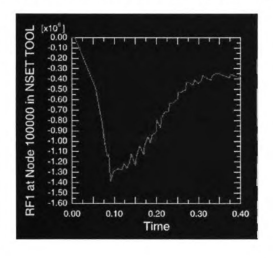
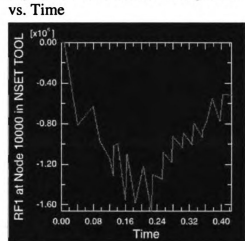


Figure 36: Mild Mesh Cutting Force



The cutting force versus time plot of the fine mesh is much smoother that the mildly refined mesh but follows a similar path. This shows the FEM model converging to a solution with mesh refinement.

### **Conclusions**

Reaction forces (cutting force and thrust force) computed by the FEM model were along the same order of magnitude as the simplified mechanics calculations. This shows that the FEM model is computing realistic values for the given machining parameters.

An increase in chip curvature can be seen as the rake angle is decreased for all three cutting speeds. Therefore, this model shows that a decrease in rake angle will increase chip curvature. This is an observed and expected phenomenon. It gives confidence that this machining model is an accurate predictor of chip curvature. This theory must be backed up with experimental data. Chip curvature gives insight to when the chip might break off and become debris. This is very important in today's automated machining processes. If a continuous chip is formed, it may interfere with other operations of the machine that is cutting the work material.

Cutting forces were seen to decrease linearly with an increase in rake angle for all three cutting speeds. It is expected that an increase in rake angle will decrease the cutting force because less of the resultant force is directed along the X-axis. Conversely, thrust forces were seen to increase linearly with an increase in rake angle for all three cutting speeds. It is expected that an increase in rake angle will increase the thrust force because more of the resultant force is directed along the Y-axis. These results give further confidence that the model is properly modeling orthogonal turning.

Both the cutting force and the thrust force increased as cutting speed was increased from 0.07 m/s to 0.10 m/s. It is expected that increasing the cutting speed will increase the reaction forces. This was not the case as the cutting speed was increased from 0.10 m/s to 0.13 m/s. This obvious modeling flaw can be explained by the chip

formation phenomenon during the simulation of the increased cutting speeds (0.10 m/s and 0.13 m/s). The simulation run with a cutting speed of 0.07 m/s yields a nice continuous chip (Figure 37) and smooth reaction forces versus time plots (Figures 38 and 39) that approach a steady state solution.

Figure 37: Continuous Chip formed at 0.07 m/s

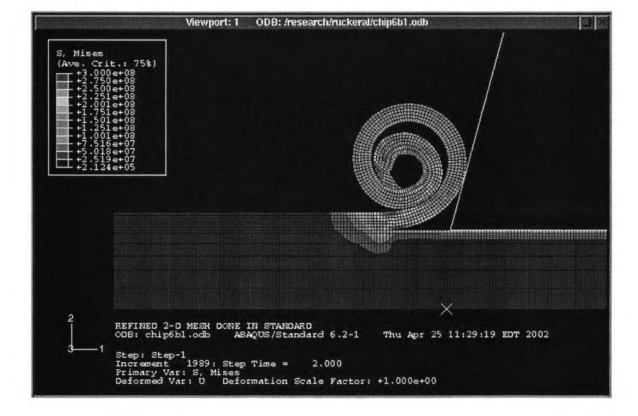


Figure 38: Cutting Force vs. Time Plot at Cutting Speed of 0.07 m/s

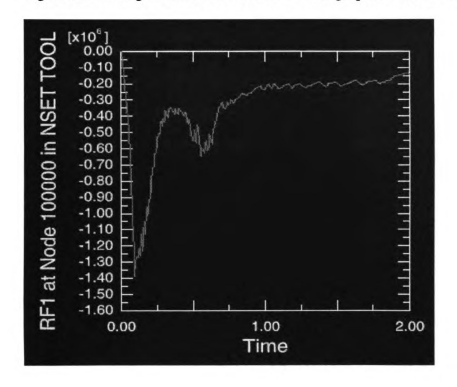
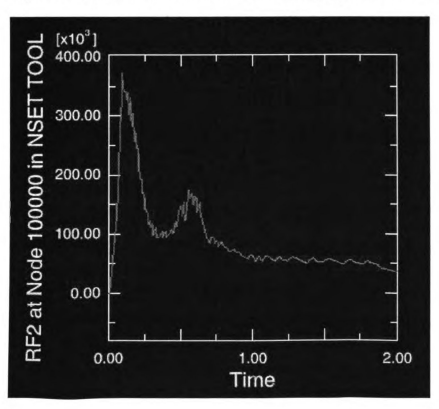


Figure 39: Thrust Force vs. Time Plot at Cutting Speed of 0.07 m/s



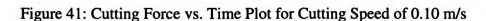
During the simulation of the faster cutting speeds of 0.10 m/s and 0.13 m/s, the chip curvature became extreme and the chip curled into the work material (Figure 39).

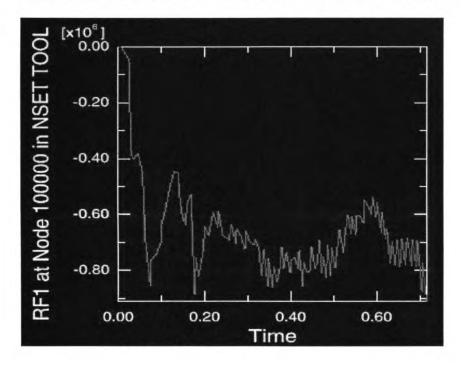
Figure 40: Chip Curled into the Work Material



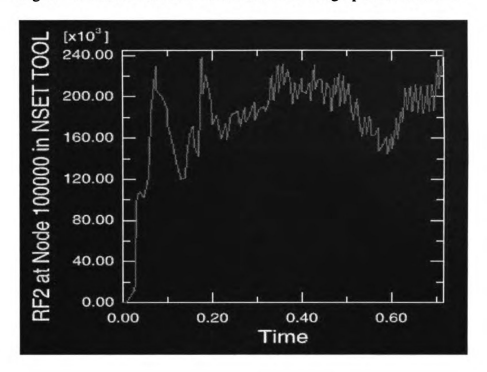
The model was defined so that the front surface of the chip could not penetrate the top surface of the chip. It was attempted to implement a similar definition so that the bottom surface of the chip could not penetrate the top surface of the chip (which is occurring in Figure 39). Such a definition was not allowed to run in ABAQUS. The extreme nature of the deformations taking place during the simulation could not be modeled for this chip thickness. A much thinner chip may yield better modeling and better results.

Also, the reaction forces vs. time plots (Figures 40 and 41) were not smooth and difficult to approximate. This is believed to be caused by the forces involved with the chip contacting itself. The results for cutting speeds of 0.10 m/s and 0.13 m/s may not be accurate.









#### Limitations and Future Work

The chip curling and penetrating into the work material at cutting speeds of 0.10 m/s and 0.13 m/s is major limitation of this finite element model. This problem affects the reliability of results.

This machining model does not include temperature and strain rate into the constitutive equation. Elastic and plastic deformation is incorporated into the model (according to Figure 9). The incorporation of these variables into a user defined constitutive equation is left for future works.

Also, the chip-separation criterion of increasing crack length with time is unrealistic to actual machining. In the future, a stress failure criterion will be incorporated for chip separation. This way, the failure plane is not defined by the user.

## References

- [1] Groover1(996). <u>Fundamentals of Modern Manufacturing</u>. Prentice-Hall Publishers. Pg:543-557
- [2] Hibbit, Karlsson, Sorensen (2001). <u>ABAQUS/Standard User's Manual Version</u> 6.2. Hibbit, Karlson, Sorensen, Inc.
- [3] Hibbit, Karlsson, Sorensen (2001). <u>ABAQUS/Explicit User's Manual Version</u>
  6.2. Hibbit, Karlson, Sorensen, Inc.
- [4] Komvopoulos, Erpenbeck (1991, August). Finite Element Modeling of Orthogonal Metal Cutting. <u>Journal of Engineering for Industry.</u> Volume 113, Pg:253-267
- [5] Lei, Shin, Incropera (1999, November). Material Constitutive Modeling Under High Strain Rates and Temperatures Through Orthogonal Machining Tests. <u>Journal of Manufacturing Science and Engineering.</u> Volume 121, Pg:577-585.
- [6] Shaw (1991). Metal Cutting Principles. Oxford University Press. Pg:11-47
- [7] Tlusty (2000). Manufacturing Processes and Equipment. Prentice-Hall Publishers. Pg:419
- [8] Kwon (2000, January). Predictive Models for Flank Wear on Coated Inserts.

  Journal of Tribology-Transactions of the ASME. Volume 122, no.1, Pg:340-347.
- [9] Obikawa, Usui (1996, May). Computational Machining of Titanium Alloy-Finite Element Modeling and a Few Results. <u>Journal of Manufacturing Science and Engineering</u>. Volume 118. Pg:208-215.

- [10] Strenkowski, Athavale (1997, November). A Partially Constrained Eulerian Orthogonal Cutting Model for Chip Control Tools. <u>Journal of Manufacturing Science and Engineering.</u> Volume 119, Pg:681-688.
- [11] Poulachon, Moisan, Jawahir (2001, November). Evaluation of Chip Morphology in Hard Turning Using Constitutive Models and Material Property Data. Proceedings of 2001 ASME International Mechanical Engineering Congress and Exposition.
- [12] Shih (1995, February). Finite Element Simulation of Orthogonal Metal Cutting.

  Journal of Engineering for Industry. Volume 117, Pg:84-93.
- [13] Strenkowski, Carroll (1985, November). A Finite Element Model of Orthogonal Metal Cutting. <u>Journal of Engineering for Industry</u>. Volume 107, Pg:349-354.
- [14] Provided by General Motors

